Atomic structure via highly charged ions and their exact quantum states

G. Friesecke[1,2] and B. D. Goddard[2]
[1] *Center for Mathematics, TU Munich, Germany*
[2] *Mathematics Institute, University of Warwick, Coventry CV47AL, UK*
(Dated: 30 December, 2009)

For highly charged ions with 3 to 10 electrons, we derive explicit, closed form quantum states which become exact in the high charge limit. When combined with suitably renormalized experimental data across iso-electronic sequences, these quantum states provide a novel and widely applicable route to predicting electronic configurations and term values for neutral atom energy levels. Moreover, our findings allow to predict missing levels, suggest that certain current term assignments for five-electron ions are incorrect, and provide insight into the rare failure of Hund's rules in excited states.

PACS numbers: 31.15.ac, 31.15.ae, 32.30.-r

It has long been recognized by experimental spectroscopists [3, 7] and quantum theorists [16, 18, 23, 24, 28] that highly charged ions provide an attractive setting for the detailed understanding of electronic structure and spectral properties of many-electron systems. Highly charged ions are also of direct interest in many contexts, e.g. strong field experiments in quantum electrodynamics [12], plasma physics [26], and the investigation of parity non-conservation [19].

Here we report, for highly charged ions with 3 to 10 electrons, explicit, closed form quantum states which become exact in the high charge limit. The ground states are surprisingly similar to the semi-empirical hydrogen orbital configurations going back to Bohr, Hund, Pauli and Slater [4, 15, 25]. Our exact quantum states provide novel insight into the fundamental mechanisms by which atomic structure emerges from quantum mechanics. In particular, they yield a new method for term and configuration assignment for neutral atoms, by using suitably renormalized experimental levels of the corresponding iso-electronic sequence, such as Li, Be^+, B^{++}, C^{+++}, ..., to interpolate to high charge ions. Also, our findings suggest that certain current term assignments for five-electron ions are incorrect, allow to predict missing levels, and offer theoretical insight into Hund's rules and their occasional failure.

I. THEORETICAL BACKGROUND

Starting point of all theoretical insight into atomic energy levels and states is the time-independent Schrödinger equation

$$H\Psi = E\Psi, \tag{1}$$

where H is the Hamiltonian of the system, E is the energy, and Ψ is the wavefunction of the electrons.

For the lighter atoms, relativistic effects can be neglected and, for nuclear charge Z and N electrons and in atomic units, the (Born-Oppenheimer) Hamiltonian is

$$H = \sum_{i=1}^{N}\Big(-\frac{1}{2}\nabla_i^2 - \frac{Z}{r_i}\Big) + \sum_{1\le i<j\le N}\frac{1}{r_{ij}}. \tag{2}$$

Here the r_i and r_{ij} are the electron-nucleus respectively electron-electron distances, and ∇_i is the gradient with respect to the position coordinates x_i of the i^{th} electron. The wavefunction Ψ depends on the position coordinates and spins of all the electrons, and must be antisymmetric with respect to simultaneous exchange of the positions and spins of any two electrons, by the Pauli principle.

II. QUANTUM STATES

Our results concern iso-electronic sequences. These are defined by holding the number N of electrons fixed, and increasing the nuclear charge Z, as in the Lithium sequence Li, Be^+, B^{++}, C^{+++}, ... We find that in the large Z limit, the low-lying quantum states can be determined explicitly, in closed form. The ground states for 1 to 10 electrons are shown in Figure I. For excited states see Table II. The status of these quantum states is given by the following mathematical theorem: *the difference between the true solutions to the Schrödinger equation (1), (2), and the simple wavefunctions given in the tables, tends in a least squares sense to zero along each iso-electronic sequence.*

The derivation of these results is outlined in an Appendix. The full details are documented elsewhere [11]. In an interesting previous study [18], such asymptotic wavefunctions are derived, but those given for B, Be, C were incorrect, being the standard hydrogen orbital configurations.

We note that the best available neutral atom or small molecule wavefunctions delivered by computational methods [14] consist of a superposition of millions [5] or even billions [8] of different (method dependent) configurations, with the exact functions requiring an infinite superposition [9]. The simplicity of the wavefunctions derived here from (1), (2) for ions is then remarkable, and lends theoretical support to the continuing use of simplified wavefunctions in the atomic spectra database [21], and their ongoing use as a source of physical and chemical intuition and a starting point for designing reduced models of complex systems [1, 6, 20, 22].

We now compare the ground states in Figure I to the

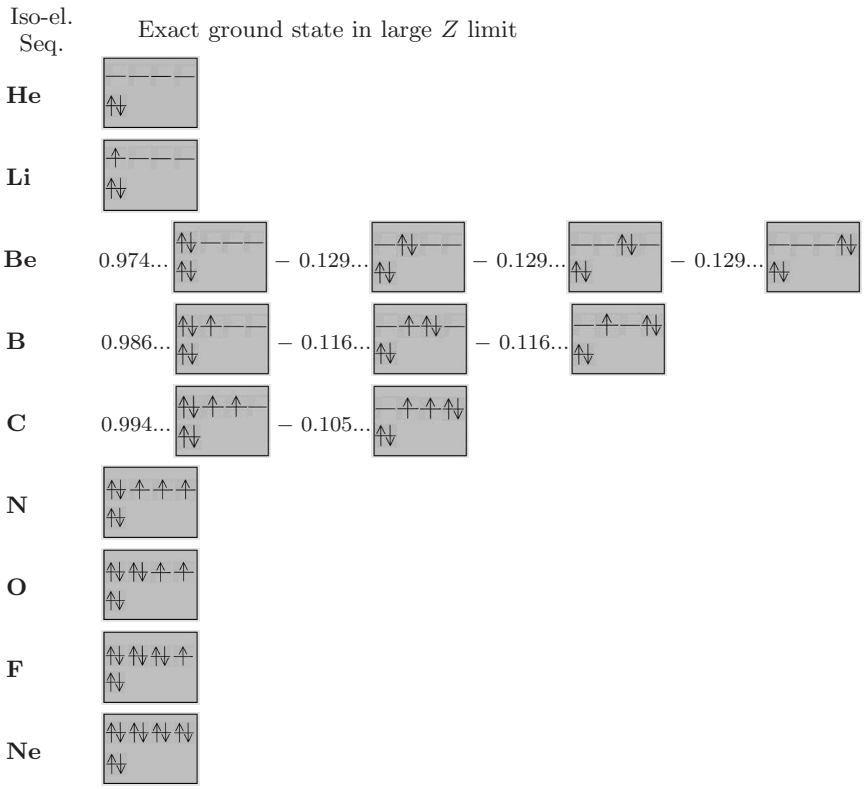

FIG. 1: Diagrammatic representation of the ground states of the Schrödinger equation (1), (2) in the large Z limit. Arrows indicate spin-up and spin-down electrons occupying the four lowest hydrogen levels ($1s$, bottom; $2s$, top left; $2p_i$, i=1,2,3, top right). Note the close similarity with the semi-empirical hydrogen orbital configurations. For more details see Table I.

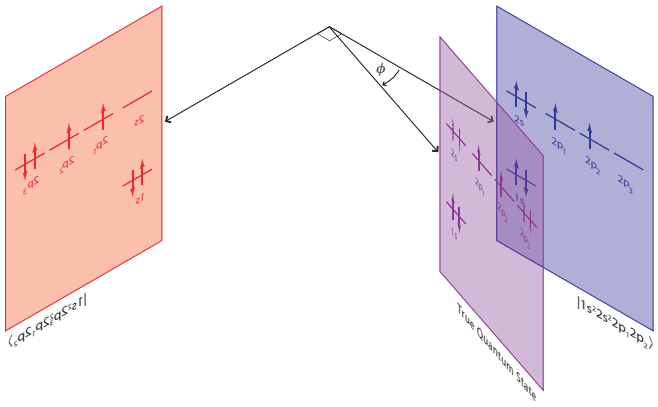

FIG. 2: Hilbert space visualization of the large-Z six-electron ion ground state. Note that it can be written in the form $\cos\phi|1s^2 2s^2 2p_1 2p_2\rangle - \sin\phi|1s^2 2p_1 2p_2 2p_3^2\rangle$, with the non-obvious angle $\phi = \arctan((\sqrt{221876564389} - 460642)/98415) \approx 6^o$.

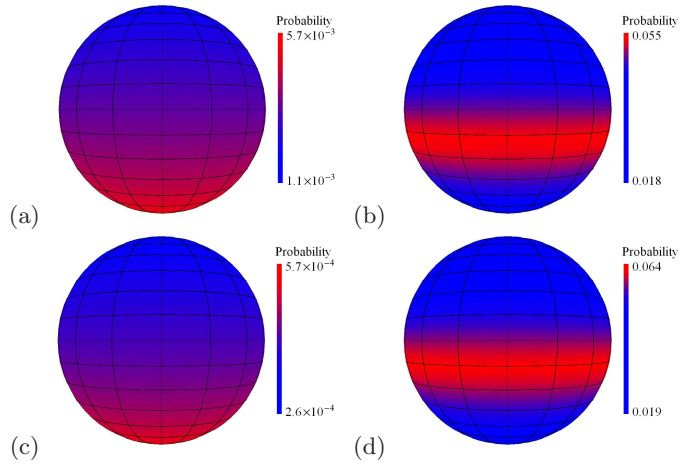

FIG. 3: Quantum probability of finding a second electron anywhere on the sphere of radius N/Z a.u. when the first electron is at the north pole, for the ground states of various atoms/ions. (a) high charge ion, Beryllium sequence; (c) neutral Beryllium; (b) high charge ion, Nitrogen sequence; (d) neutral Nitrogen. Plots (a) and (b) show exact pair densities $\rho_2(x,y) = \langle\Psi|\delta(x-x_1)\delta(y-x_2)|\Psi\rangle$, Ψ from Table I, $x = (0,0,N/Z)$, $|y| = N/Z$; (c) and (d) are based on numerical wavefunctions [10]. In (a), neglecting the corrections in Table I and Fig. 1 to the standard $1s^2 2s^2$ configuration would lead to the unphysical result of a constant probability.

semi-empirical hydrogen orbital configurations developed by Bohr, Hund and Slater [4, 15, 25] to explain the periodic table. Recall the underlying rules: (a) Each electron in an atom occupies a hydrogenic orbital.[29] (b) The orbitals in each hydrogen energy level, or shell, form sub-shells which are occupied in the order $1s$ $2s$ $2p$ $3s$

Iso-el. Seq.	Sym.	Exact ground state in large Z limit	Dim.
H	^2S	$\|1s\rangle$, $\|\overline{1s}\rangle$	2
He	^1S	$\|1s^2\rangle$	1
Li	^2S	$\|1s^2 2s\rangle$, $\|1s^2\overline{2s}\rangle$	2
Be	^1S	$\frac{1}{\sqrt{1+c^2}}\Big(\|1s^2 2s^2\rangle + c\frac{1}{\sqrt{3}}\big(\|1s^2 2p_1^2\rangle + \|1s^2 2p_2^2\rangle + \|1s^2 2p_3^2\rangle\big)\Big)$ $c = -\frac{\sqrt{3}}{59049}(2\sqrt{1509308377} - 69821) = -0.2310995\ldots$	1
B	$^2P^o$	$\frac{1}{\sqrt{1+c^2}}\Big(\|1s^2 2s^2 2p_i\rangle + c\frac{1}{\sqrt{2}}\big(\|1s^2 2p_i 2p_j^2\rangle + \|1s^2 2p_i 2p_k^2\rangle\big)\Big)$ $\frac{1}{\sqrt{1+c^2}}\Big(\|1s^2 2s^2\overline{2p_i}\rangle + c\frac{1}{\sqrt{2}}\big(\|1s^2\overline{2p_i}2p_j^2\rangle + \|1s^2\overline{2p_i}2p_k^2\rangle\big)\Big)$ $(i,j,k) = (3,1,2),(1,2,3),(2,3,1)$ $c = -\frac{\sqrt{2}}{393660}(\sqrt{733174301809} - 809747) = -0.1670823\ldots$	6
C	^3P	$\frac{1}{\sqrt{1+c^2}}\big(\|1s^2 2s^2 2p_i 2p_j\rangle + c\|1s^2 2p_k^2 2p_i 2p_j\rangle\big)$ $\frac{1}{\sqrt{1+c^2}}\Big(\frac{1}{\sqrt{2}}\big(\|1s^2 2s^2 2p_i\overline{2p_j}\rangle + \|1s^2 2s^2\overline{2p_i}2p_j\rangle\big)$ $+c\frac{1}{\sqrt{2}}\big(\|1s^2 2p_k^2 2p_i\overline{2p_j}\rangle + \|1s^2 2p_k^2\overline{2p_i}2p_j\rangle\big)\Big)$ $\frac{1}{\sqrt{1+c^2}}\big(\|1s^2 2s^2\overline{2p_i 2p_j}\rangle + c\|1s^2 2p_k^2\overline{2p_i 2p_j}\rangle\big)$ $(i,j,k) = (3,1,2),(1,2,3),(2,3,1)$ $c = -\frac{1}{98415}(\sqrt{221876564389} - 460642) = -0.1056317\ldots$	9
N	$^4S^o$	$\|1s^2 2s^2 2p_1 2p_2 2p_3\rangle$ $\frac{1}{\sqrt{3}}(\|1s^2 2s^2\overline{2p_3}2p_1 2p_2\rangle + \|1s^2 2s^2 2p_3\overline{2p_1}2p_2\rangle + \|1s^2 2s^2 2p_3 2p_1\overline{2p_2}\rangle)$ $\frac{1}{\sqrt{3}}(\|1s^2 2s^2\overline{2p_3 2p_1}2p_2\rangle + \|1s^2 2s^2\overline{2p_3}2p_1\overline{2p_2}\rangle + \|1s^2 2s^2 3\overline{2p_1 2p_2}\rangle)$ $\|1s^2 2s^2\overline{2p_1 2p_2 2p_3}\rangle$	4
O	^3P	$\|1s^2 2s^2 2p_i^2 2p_j 2p_k\rangle$ $\frac{1}{\sqrt{2}}(\|1s^2 2s^2 2p_i^2 2p_j\overline{2p_k}\rangle + \|1s^2 2s^2 2p_i^2\overline{2p_j}2p_k\rangle)$ $\|1s^2 2s^2 2p_i^2\overline{2p_j 2p_k}\rangle$ $(i,j,k) = (3,1,2),(1,2,3),(2,3,1)$	9
F	$^2P^o$	$\|1s^2 2s^2 2p_i^2 2p_j^2 2p_k\rangle$ $\|1s^2\overline{22}2p_i^2 2p_j^2\overline{2p_k}\rangle$ $(i,j,k) = (3,1,2),(1,2,3),(2,3,1)$	6
Ne	^1S	$\|1s^2 2s^2 2p_1^2 2p_2^2 2p_3^2\rangle$	1

TABLE I: An orthonormal basis of ground states of the Schrödinger equation (1), (2) in the large Z limit, in standard notation (see Appendix). The symmetry agrees with experiment for each element of each sequence, including neutral atoms.

$3p$ $4s$ $3d$ .... (c) *Hund's rule* Within any partially filled sub-shell, the electrons adopt a configuration with the greatest possible number of aligned spins. Thus, in, say, the Carbon sequence the six electrons would occupy the orbitals $1s\,\overline{1s}\,2s\,\overline{2s}\,2p_1\,2p_2$ (the alternative choices $\overline{2p_1}$ or $\overline{2p_2}$ for the last orbital are consistent with (b) but not (c)).

There is a long history of explaining this beautiful heuristic picture in terms of numerical solutions of Hartree- and Hartree-Fock models [13]; here, for highly charged ions it is seen to emerge directly from the fundamental laws of quantum mechanics. For seven out of ten elements, the high-charge limit of the Schrödinger ground state (Figure I) coincides with the hydrogen orbital configuration predicted from (a), (b), (c). For the remaining three elements Be, B, C, the large-ion ground state contains the hydrogen orbital configuration as a dominant part; but a ten to twenty percent admixture of a particular "higher sub-shell" configuration is also present, in which the $2s^2$ electron pair has migrated to a $2p$ orbital. This shows that rule (b) is not obeyed in a strict sense, but only probabilistically. Numerical ab initio computations confirm that this effect persists as Z is decreased to neutrality [10].

These higher sub-shell contributions turn out to significantly affect the typical *relative position of electron pairs*, which, as we argue below, is a significant indicator for preferred bond angles and hence chemical behaviour.

Figure 3 demonstrates this point for the Beryllium sequence. For the quantum state in Figure I, and the first electron fixed, without loss of generality, at the north pole on a sphere around the nucleus, the preferred position of the second electron (red) is seen to be at the south pole; but all positions would be equally likely when the higher subshell contributions are ignored. It is interesting to compare with the Nitrogen sequence, where the preferred position of the second electron (red) is at a nonlinear angle. This different behaviour of Be and N correlates in a

tantalizing way with the experimental fact that the BeH_2 molecule is straight, but NH_2 is bent. The connection becomes clear when one interprets the shape of the trimer as a rough measurement of the relative position of the two bonding electrons contributed by the central atom.

Our exact quantum states also allow theoretical insight into the failure of Hund's rules for certain excited states. Experimentally, the lowest $1s^2 2s2p^3\ ^3S^o$ and $^1D^o$ levels of the Carbon sequence cross between $Z = 20$ and $Z = 19$, whereas Hund's rules would order them universally as $^3S^o < {}^1D^o$. However, the energy difference as read off from Table II (by writing each energy as $\langle\Psi|H|\Psi\rangle$ and using Slater's rules [14]) consists of a $2s$–$2p$ positive exchange term and a $2p$–$2p$ negative exchange term, $E_{^3S^o} - E_{^1D^o} = (2s2p_1|2p_1 2s) - 3(2p_1 2p_2|2p_2 2p_1)$, and so indeed could have either sign, depending on the orbitals. This interesting effect is missed when these states are modelled by the aufbau principle Slater determinants $|1s^2 2s2p_3\overline{2p_1 2p_2}\rangle$ (singlet) and $|1s^2 2s2p_3 2p_1\overline{2p_2}\rangle$ (triplet). The energy difference is then $E_{^3S^o} - E_{^1D^o} = -(2s2p_1|2p_1 2s) < 0$, which wrongly predicts a universal ordering.

III. ENERGY LEVELS

The energy levels $E = E_j(N, Z)$ of the atom/ion with N electrons and nuclear charge Z have the the following asymptotic expansion for large Z [11, 16, 23, 24, 28]

$$E_j(N, Z) = a^{(0)}(N)Z^2 + a_j^{(1)}(N)Z + \mathcal{O}(1). \qquad (3)$$

Here $a^{(0)}(N)Z^2$ is a contribution purely from kinetic energy and electron-nucleus attraction, whilst the next order term $a_j^{(1)}(N)Z$ stems from electron-electron repulsion. The coefficient $a^{(0)}$ is a sum of hydrogen atom eigenvalues, $a^{(0)}(N) = \sum_{i=1}^{N} -1/n_i^2$; for the ground state one has $a^{(0)}_{\rm GS}(N) = -1 - (N-2)/8$ for $N = 2, \ldots, 10$. Much less trivially, we have succeeded in also determining $a_j^{(1)}$ in closed form, for all low-lying energy levels of the first 10 atoms (see Table II and the Appendix). We note that the O(1) term in (3) can be expanded further into

$$a_j^{(2)}(N) + a_j^{(3)}(N)\tfrac{1}{Z} + ...; \qquad (4)$$

but already the next order coefficients $a_j^{(2)}(N)$ are not known exactly even for $N = 2$ (for numerical values see e.g. [2]). Hence our closed-form energies $a^{(0)}(N)Z^2 + a_j^{(1)}(N)Z$, unlike our closed-form wavefunctions, do not have an asymptotically vanishing absolute error, but only an asymptotically vanishing relative error.

To compare the asymptotic result (3) to experimental energy levels, we argue that it is useful not to make a comparison of bare values, or bare gaps, but to first *renormalize* both the energy gaps and the nuclear charge Z so as to make them constant at $Z = \infty$. We see from (3) that this is achieved by the following prescription:

$$\begin{gathered}\text{Do not plot } E_j(Z) - E_1(Z) \text{ against } Z,\\ \text{but } \tfrac{E_j(Z)-E_1(Z)}{Z^2} \text{ against } \tfrac{1}{Z}.\end{gathered} \qquad (5)$$

This scaling, which is a natural application of "renormalization group thinking", also reveals a wealth of hidden structure in the experimental spectra.

Theoretical predictions from (3) and Table II are:

(i) The energy levels should form smooth curves as a function of $1/Z$ This is a consequence [17] of the smooth dependence of the Hamiltonian (2) on Z, and smoothness of the rescaling (5).

(ii) The number of curves converging to zero as $1/Z \to 0$ should correspond exactly to the number $n(N)$ of different $a_j^{(1)}$ possible in formula (3) when $a^{(0)}$ is given by its lowest value $a^{(0)}_{\rm GS}$. By our results, $n(N)$ equals the number of eigenvalues of the reduced Hamiltonian (6) (for $2 \le N \le 10$, $1, 2, 6, 8, 12, 8, 6, 2, 1$).

(iii) The exact theoretical tangents at $1/Z = 0$ to the energy gap curves are given by $t_j(\frac{1}{Z}) = (a_j^{(1)}(N) - a_1^{(1)})/Z$, with the $a_j^{(1)}$ as in Table II.

(iv) Energy curves whose dominant configurations contain higher principal quantum number orbitals should converge to values greater than zero as $1/Z \to 0$, more explicitly to $a^{(0)}(N) - a^{(0)}_{\rm GS}(N)$.

These predictions are all beautifully confirmed by the experimental data, see Figure 4.

Such plots (see Figure 3 (h)) also clearly demonstrate, for $Z \gtrsim 20$, relativistic deviations from (1),(2) (theoretically, energy corrections scale like $\alpha^2 Z^4$ as Z gets large, where $\alpha \approx 1/137$ is the fine structure constant).

Finally we discuss the error made by neglecting the higher order asymptotic energy corrections in (4). As Fig. 4 and Table II demonstrate, further terms are not needed to resolve the number of levels emanating from the non-interacting ground state, along with their term values and orderings. The size of the next order O(1) term is known numerically in some cases, such as the asymptotically lowest (^1S, dominant configuration $1s^2 2s^2$), third ($^1P^o$, domin. conf. $1s^2 2s2p$) and sixth (^1S, domin. conf. $1s^2 2p^2$) levels of the Be sequence in Fig. 4(b) [27]:

Gap	$^1P^o$–^1S	^1S–^1S	$^1P^o$–^1S	^1S–^1S
Z	4	4	20	20
$O(Z^2)$+O(Z) contrib. [11]	0.4939	0.9252	2.4693	4.6260
O(1) contrib. [27]	-0.2103	-0.3638	-0.2103	-0.3638
Experimental value [21]	0.1939	0.3471	2.3630	4.4068

Thus the O(1) term in (4) is important for neutral atoms, as expected, while for highly charged ions with Z≈20, the error with or without this term is of the same magnitude (e.g. -0.104 versus +0.106 for the $^1P^o$–^1S Be sequence gap). Hence in order to significantly improve our theoretical energies in this regime, relativistic effects would need to be taken into account as well.

Term	Ψ	$E(Z)$
${}^3P$	$\frac{1}{\sqrt{1+c^2}}\left(\|1s\overline{1s}2s\overline{2s}2p_1 2p_2\rangle + c\|1s\overline{1s}2p_3\overline{2p_3}2p_1 2p_2\rangle\right)$ $c=\frac{460642}{98415}-\frac{\sqrt{221876564389}}{98415}$	$-\frac{3}{2}Z^2+\left(\frac{3806107}{1119744}-\frac{\sqrt{221876564389}}{3359232}\right)Z$
${}^1D$	$\frac{1}{\sqrt{1+c^2}}\Big(\frac{1}{\sqrt{6}}\left(2\|1s\overline{1s}2s\overline{2s}2p_3\overline{2p_3}\rangle-\|1s\overline{1s}2s\overline{2s}2p_1\overline{2p_1}\rangle-\|1s\overline{1s}2s\overline{2s}2p_2\overline{2p_2}\rangle\right)$ $+c\frac{1}{\sqrt{6}}\left(2\|1s\overline{1s}2p_1\overline{2p_1}2p_2\overline{2p_2}\rangle-\|1s\overline{1s}2p_3\overline{2p_3}2p_1\overline{2p_1}\rangle-\|1s\overline{1s}2p_3\overline{2p_3}2p_2\overline{2p_2}\rangle\right)\Big)$ $c=-\frac{460642}{98415}+\frac{\sqrt{221876564389}}{98415}$	$-\frac{3}{2}Z^2+\left(\frac{19148633}{5598720}-\frac{\sqrt{221876564389}}{3359232}\right)Z$
${}^1S$	$\frac{1}{\sqrt{1+c^2}}\Big(\frac{1}{\sqrt{3}}\left(\|1s\overline{1s}2s\overline{2s}2p_3\overline{2p_3}\rangle+\|1s\overline{1s}2s\overline{2s}2p_1\overline{2p_1}\rangle+\|1s\overline{1s}2s\overline{2s}2p_2\overline{2p_2}\rangle\right)$ $+c\Big(\frac{1}{\sqrt{3}}\left(\|1s\overline{1s}2p_3\overline{2p_3}2p_1\overline{2p_1}\rangle+\|1s\overline{1s}2p_3\overline{2p_3}2p_2\overline{2p_2}\rangle+\|1s\overline{1s}2p_1\overline{2p_1}2p_2\overline{2p_2}\rangle\right)\Big)\Big)$ $c=\frac{230321}{98415}-\frac{\sqrt{62733275266}}{98415}$	$-\frac{3}{2}Z^2+\left(\frac{966289}{279936}-\frac{\sqrt{62733275266}}{1679616}\right)Z$
${}^5S^o$	$\|1s\overline{1s}2s2p_3 2p_1 2p_2\rangle$	$-\frac{3}{2}Z^2+\frac{464555}{139968}Z$
${}^3D^o$	$\frac{1}{\sqrt{6}}\left(2\|1s\overline{1s}2s\overline{2p_3}2p_1 2p_2\rangle-\|1s\overline{1s}2s2p_3 2p_1\overline{2p_2}\rangle-\|1s\overline{1s}2s2p_3\overline{2p_1}2p_2\rangle\right)$	$-\frac{3}{2}Z^2+\frac{4730843}{1399680}Z$
${}^3P^o$	$\frac{1}{\sqrt{2}}\left(\|1s\overline{1s}2s2p_3 2p_1\overline{2p_1}\rangle+\|1s\overline{1s}2s2p_3 2p_2\overline{2p_2}\rangle\right)$	$-\frac{3}{2}Z^2+\frac{1904147}{559872}Z$
${}^3S^o$	$\frac{1}{\sqrt{12}}\left(3\|1s\overline{1s}2s\overline{2s}2p_3 2p_2 2p_2\rangle-\|1s\overline{1s}2s\overline{2p_3}2p_1 2p_2\rangle\right.$ $\left.-\|1s\overline{1s}2s2p_3\overline{2p_1}2p_2\rangle-\|1s\overline{1s}2s2p_3 2p_1\overline{2p_2}\rangle\right)$	$-\frac{3}{2}Z^2+\frac{961915}{279936}Z$
${}^1D^o$	$\frac{1}{\sqrt{12}}\left(2\|1s\overline{1s}2s2p_3\overline{2p_1 2p_2}\rangle-\|1s\overline{1s}2s\overline{2p_3}2p_1\overline{2p_2}\rangle-\|1s\overline{1s}2s\overline{2p_3}2p_1 2p_2\rangle\right.$ $\left.+2\|1s\overline{1s2s2p_3}2p_1 2p_2\rangle-\|1s\overline{1s2s}2p_3 2p_1\overline{2p_2}\rangle-\|1s\overline{1s2s}2p_3\overline{2p_1}2p_2\rangle\right)$	$-\frac{3}{2}Z^2+\frac{9625711}{2799360}Z$
${}^1P^o$	$\frac{1}{2}\left(\|1s\overline{1s}2s\overline{2p_3}2p_1\overline{2p_1}\rangle-\|1s\overline{1s2s}2p_3 2p_1\overline{2p_1}\rangle\right.$ $\left.+\|1s\overline{1s}2s\overline{2p_3}2p_2\overline{2p_2}\rangle-\|1s\overline{1s2s}2p_3 2p_2\overline{2p_2}\rangle\right)$	$-\frac{3}{2}Z^2+\frac{242119}{69984}Z$
${}^3P$	Same as ${}^3P$ above, $c=\frac{460642}{98415}+\frac{\sqrt{221876564389}}{98415}$	$-\frac{3}{2}Z^2+\left(\frac{3806107}{1119744}+\frac{\sqrt{221876564389}}{3359232}\right)Z$
${}^1D$	Same as ${}^1D$ above, $c=-\frac{460642}{98415}-\frac{\sqrt{221876564389}}{98415}$	$-\frac{3}{2}Z^2+\left(\frac{19148633}{5598720}+\frac{\sqrt{221876564389}}{3359232}\right)Z$
${}^1S$	Same as ${}^1S$ above, $c=\frac{230321}{98415}+\frac{\sqrt{62733275266}}{98415}$	$-\frac{3}{2}Z^2+\left(\frac{966289}{279936}+\frac{\sqrt{62733275266}}{1679616}\right)Z$

TABLE II: The twelve lowest asymptotic eigenstates of (1), (2) for the Carbon sequence ($N=6$), along with their term values and energies, ordered from top to bottom with increasing energy. The theoretical large-Z ordering agrees with experiment for all $Z\geq 20$, and differs by a single crossing between the 7th and 8th level when $Z\leq 19$ (see Fig. 4(d)). Only the states with $L_3=0$ and $S_3=S$ are shown. The remaining states, and those for the remaining $N=3,...,10$, are listed in [11].

IV. TERM AND CONFIGURATION ASSIGNMENT FOR NEUTRAL ATOMS

We now turn to neutral atoms and the important issue of assigning term values (total spin, angular momentum and parity quantum numbers L, S and p, encoded as ${}^{2S+1}X^{\nu}$, where ν indicates parity and $X=S,P,D,...$ means $L=0,1,2,...$) to observed energy levels.

We propose an alternative to standard assignment methods [6], which carefully exploits both experimental and theoretical insights on the large Z limit.
(1) Plot the experimental excitation energies along an isoelectronic sequence, under the scaling (5), as in Fig.4.
(2) Near $1/Z=0$ our exact results (see Table II) deliver closed-form wavefunctions for each level, and hence unambiguous term values and configurations.
(3) The term values remain constant along each energy level curve, since L, S and p are quantized and hence their continuous dependence on the parameter Z forbids them to change.
(4) Ambiguities arise only when continuing term assignments through level crossings. These can be resolved by a simple and theoretically justified curvature minimization algorithm, described below.

We have applied this method to the 45 energy levels emanating from the ground states of the atoms Li to Ne at $1/Z=0$, obtaining the experimentally established term value in each (!) case. For the corresponding ions, our method captured correctly the crossings in the Carbon sequence between $Z=19$ and 20, the Beryllium sequence between $Z=4$ and 5, and the non-crossing despite visual ambiguity in the Boron sequence between $Z=5$ and 6.

Our method also assigns a definite 'configuration' (e.g. $1s^2 2s^2 2p^3$) to an atomic quantum state: namely *the configuration associated to the corresponding energy level curve in the limit 1/Z→0.* This procedure can be thought of as an alternative, less empirical definition of the notion of configuration: not as an approximate property of the state (obtained as a best fit of experimental data to model wave functions), but as an exact property of the deformed state which emerges when one makes the nuclear charge large.

Our curvature minimization algorithm (4) continues term assignment iteratively from Z to $Z-1$ by considering an arbitrary possible pairing of levels at Z with those at $Z-1$, connecting each pair by a cubic spline

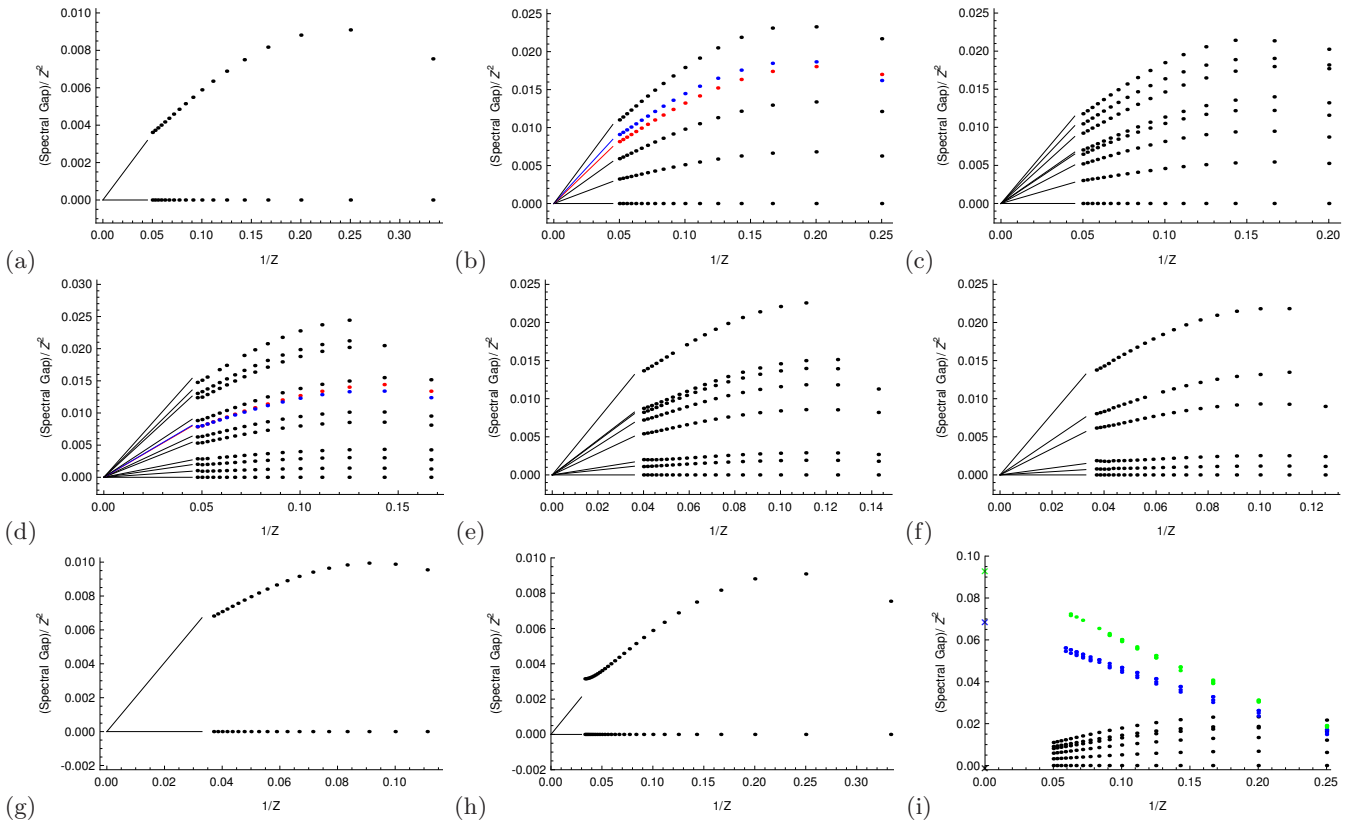

FIG. 4: (a)–(g): Energy levels of the iso-electronic sequences with three to nine electrons. Lines: asymptotic Schrödinger levels (this paper); points: experimental data [21] (averaged, by multiplicity, over J); only levels associated to $1s^2 2s^i 2p^{N-2-i}$ configurations are shown. To reveal the close similarity of spectra across each iso-electronic sequence, the natural but previously unused scaling (5) is essential. Note that only two level crossings are present (in the Beryllium and Carbon sequences, coloured red and blue). (h): Relativistic effects in the Lithium sequence for $Z \gtrsim 20$. (i): Higher principal quantum number levels in the Beryllium sequence and their theoretical limits (5/72 for $1s^2 2s^2 3\ell$ and 3/22 for $1s^2 2s^2 4\ell$, $\ell = s, p$; blue and green points and crosses respectively).

$\tilde{E}_i(s)$ $(Z-1 \le s \le Z)$, and minimizing the resulting total level curvature $C(Z-1, Z) = \int_{Z-1}^{Z} \sum_{i=1}^{N} (\tilde{E}_i''(s))^2 ds$ over all matchings. This algorithm has its theoretical basis in the following simple mathematical result: with the $\tilde{E}_i$ replaced by the exact Schrödinger levels, and assuming any crossings are transverse, C is finite only for the correct labelling, and infinite otherwise, due to kink singularities at crossings. In practice, we found it sufficient to interpolate by cubic splines.

This method also allows the prediction of missing experimental values, by taking the value given by the cubic spline at the appropriate value of $1/Z$. See Figure 4. Due to the lack of constraints for the cubic spline fitting, 'end' values at $Z = N$ are harder to predict, as indicated by the error bar for the Carbon levels.

N	Z	Atom/Ion	Domin.Conf.	Sym.	$E_i - E_1$ (au)
6	15	P X	$1s^2 2p^4$	^1S	4.0831
6	18	Ar XIII	$1s^2 2p^4$	^1S	5.2334
6	18	Ar XIII	$1s^2 2s 2p^3$	$^5S^o$	0.9715
6	6	C	$1s^2 2s^2 2p^2$	^3P	0.68±0.004
6	6	C	$1s^2 2s^2 2p^2$	^1D	0.76±0.004
6	6	C	$1s^2 2s^2 2p^2$	^1S	0.85±0.004
7	18	Ar XII	$1s^2 2s 2p^4$	$^2P^o$	5.3458
8	17	Cl X	$1s^2 2s 2p^5$	$^1P^o$	3.0407

TABLE III: Missing experimental energy levels predicted from Fig. 4, along with their symmetry and the dominant configuration.

V. CORRECTION OF EXPERIMENTAL TERM ASSIGNMENTS

Our results strongly suggest that two levels of the 5-electron iso-electronic sequence are incorrectly assigned in the NIST database [21]. The levels in question are assigned to the $1s^2 2s 2p^2$ configuration, with term values ^2S $J = 1/2$ and ^2P $J = 1/2, 3/2$. For $Z \le 22$, the two $J = 1/2$ terms (experimentally indistinguishable through multiplicity) are assigned with $^2S < {}^2P$, whereas for $Z \ge 23$ (the ions V XIX, Cr XX, Mn XXI, Fe XXII, Co XXIII,

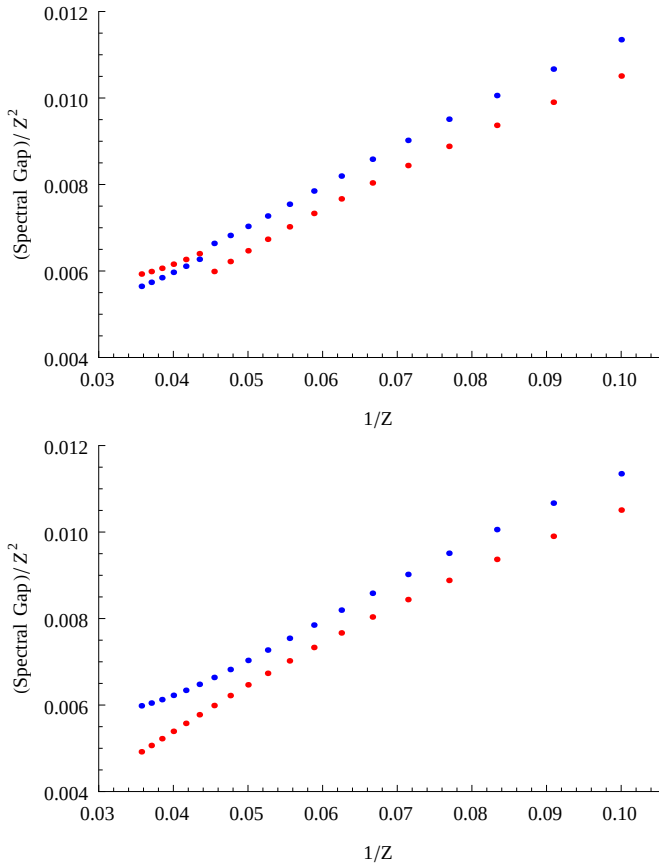

FIG. 5: Experimental energies of 5-electron ions as assigned by NIST, averaged over J (top), and with the ^2S and ^2P $J = 1/2$ levels transposed for $Z \geq 23$ before averaging (bottom). The NIST assignment appears to be at odds with the principle that the levels should lie on smooth curves.

Ni XXIV) the order is reversed. We suggest here that this reversal is incorrect; the modified data gives much more convincingly smooth curves. By contrast, the analogous ^2S and ^2P levels of seven-electron ions with configuration $1s^2 2s 2p^4$ appear to be correctly assigned.

VI. CONCLUSIONS

For highly charged ions, hydrogen orbital configurations do not just arise as semi-empirical approximations, but as exact quantum states, which emerge directly from the Schrödinger equation along with definite term values, energetic orderings, and same-shell-higher-subshell corrections. These states, when combined with the systematic study of properties of interest across iso-electronic sequences, provide a novel and widely applicable route to accessing atomic structure and complex spectra. Another use of our results, as rare benchmark data for the design of computational methods, will be explored elsewhere [10].

VII. APPENDIX

A. Notation

In Figure I, $1s$, $2s$, $2p_i$ (i=1,2,3) are the usual hydrogen orbitals for ions with nuclear charge Z and one electron, $1s(x) = Z^{3/2}e^{-Z|x|}/\sqrt{\pi}$, $2s(x) = Z^{3/2}(1 - Z|x|/2)e^{-Z|x|/2}/\sqrt{8\pi}$, $2p_i(x) = Z^{5/2}(x \cdot e_i)e^{-Z|x|/2}/\sqrt{32\pi}$. Note that the diameter of the orbitals is smaller by a factor $1/Z$ as compared to those in neutral hydrogen atoms. Here x is a 3D position coordinate, e_1, e_2, e_3 are orthonormal basis vectors of 3D space, the overbar or its absence gives the spin state (down respectively up), a square (as in $1s^2$) indicates that both spin states are occupied, and $|\varphi_1 ... \varphi_N\rangle$ stands for the Slater determinant of the orbitals φ_1,..,φ_N.

B. Reduction to a finite-dimensional problem

Use of re-scaled position coordinates $\tilde{x} = Z^{-1}x$ removes the factor Z from (2) and creates a small factor, $1/Z$, in front of electron interaction. Applying degenerate first order perturbation theory and scaling back to the original variables yields that for large Z, the lowest eigenvalues and eigenstates of (1), (2) have the asymptotic expansion (3), $\Psi = \Psi_j(N,Z) = \Phi_j^{(0)}(N,Z) + O(Z^{-1})$, where the approximate Schrödinger levels $a^{(0)}Z^2 + a_j^{(1)}Z$ and states $\Phi_j^{(0)}$ are the exact eigenvalues and eigenstates of the finite-dimensional reduced problem

$$(a')\ \ PHP\Psi = E\Psi, \quad (b')\ \ \Psi \in V_0. \tag{6}$$

Here $P = \sum_i |\Psi_i\rangle\langle\Psi_i|$ is the projector onto the non-interacting ground state V_0 (lowest eigenspace of (2) with second term deleted). Rule (b') is the same as (a) in the Aufbau principle, while (a') replaces the empirical postulates (b) and (c), instead selecting the correct hydrogen orbital configurations from theory.

C. Determining the eigenvalues and eigenstates of the reduced Hamiltonian PHP

For $2 \leq N \leq 10$, by hydrogen atom theory plus the theory of non-interacting fermions V_0 has a basis $\{\Psi_1, .., \Psi_{d(N)}\}$ of Slater determinants with hydrogen orbital configurations $(1s)^2(2s)^j(2p)^{N-2-j}$, $j = 0, 1, 2$ and dimension d= $\binom{8}{N-2}$ corresponding to the number of possible assignments of the $N-2$ valence electrons to the 8 valence orbitals. PHP is a d×d matrix with entries $\langle\Psi_i|H|\Psi_j\rangle$ (for the Carbon sequence, a 70×70 matrix whose entries are integrals over $\mathbb{R}^{18} \times \mathbb{Z}_2^6$). By conservation of total spin, angular momentum and parity under (2) (and (6)), PHP leaves the simultaneous eigenspaces of $\underline{L}^2$, L_3, $\underline{S}^2$, S_3, and parity invariant. Aided by representation theory for the underlying symmetry group

$SO(3) \times \mathbb{Z}_2 \times SU(2)$ of (1), (2), (6) (which corresponds to rotation and inversion of electron positions and rotation of spins) these can be explicitly determined [11] (for previous analysis of some cases see [6]). The largest such spaces turn out to be 2D! Evaluating the matrix elements of PHP is achieved by successively reducing the domain of integration from $\mathbb{R}^{3N}$ to $\mathbb{R}^6$ to $\mathbb{R}^3$ to $\mathbb{R}$ via Slater's rules [14], Fourier analysis, and spherical polar coordinates, and evaluating the remaining one-dimensional integrals by residue calculus as implemented in MAPLE.

[1] P. Atkins. *Physical Chemistry*. Oxford University Press, 2001.

[2] J.D. Baker, D.E. Freund, R.N. Hill, and J.D. Morgan III. Radius of convergence and analytic behavior of the 1/Z expansion. *Phys. Rev. A*, 41(3):1247–1273, 1990.

[3] H. F. Beyer, H.-J. Kluge, and V. P. Shevelko. *X-ray radiation of highly charged ions*. Springer, 1997.

[4] N. Bohr. *The Theory of Atomic Spectra and Atomic Constitution*. Cambridge University Press, 1922.

[5] B. Bories, D. Maynau, and M.-L. Bonnet. Selected excitation for CAS-SDCI calculations. *J. Comput. Chem.*, 28:632643, 2006.

[6] E. U. Condon. *Atomic Structure*. Cambridge University Press, 1980.

[7] Fred J. Currell. *The physics of multiply and highly charged ions. Vols. I & II*. Springer, 2003.

[8] H. Dachsel, R.J. Harrison, and D.A. Dixon. Multireference Configuration Interaction calculations on Cr_2: Passing the one billion limit in MRCI/MRACPF calculations. *J. Phys. Chem.*, 103:152–155, 1999.

[9] G. Friesecke. On the infinitude of non-zero eigenvalules of the single-electron density matrix for atoms and molecules. *Proc. R. Soc. Lond. A*, 459:47–52, 2003.

[10] G. Friesecke and B. D. Goddard. Asymptotics-based CI models for atoms: properties, exact solution of a minimal model for Li to Ne, and application to atomic spectra. *Multiscale Model. Simul.*, to appear, 2009.

[11] G. Friesecke and B. D. Goddard. Explicit large nuclear charge limit of electronic ground states for Li, Be, B, C, N, O, F, Ne and basic aspects of the periodic table. *SIAM J. Math. Analysis*, 41(2):631–664, 2009.

[12] S Fritzsche, P Indelicato, and Th Stohlker. Relativistic quantum dynamics in strong fields: photon emission from heavy, few-electron ions. *Journal of Physics B: Atomic, Molecular and Optical Physics*, 38(9):S707–S726, 2005.

[13] C. Froese Fischer. *The Hartree-Fock Method for Atoms. A Numerical Approach.* Wiley-Interscience, 1977.

[14] T. Helgaker, P. Joergensen, and J. Olsen. *Molecular Electronic Structure Theory*. Wiley, 2000.

[15] F. Hund. Zur deutung verwickelter spektren, insbesondere der elemente scandium bis nickel. *Zeitschrift für Physik*, 33:345–371, 1925.

[16] E. A. Hylleraas. Über der Grundterm der Zweielecktronenprobleme von H^-, He, Li^+, Be^{++} usw. *Z. Phys.*, 65:209–225, 1930.

[17] T. Kato. *Perturbation Theory for Linear Operators*. Springer, 1967.

[18] D. Layzer. On a screening theory of atomic spectra. *Annals of Physics*, 8:271–296, 1959.

[19] M. Maul, A. Schäfer, W. Greiner, and P. Indelicato. Prospects for parity-nonconservation experiments with highly charged heavy ions. *Phys. Rev. A*, 53(6):3915–3925, Jun 1996.

[20] D. Pettifor. *Bonding and structure of molecules and solids*. Oxford University Press, 1995.

[21] Yu. Ralchenko, F.-C. Jou, D.E. Kelleher, A.E. Kramida, A. Musgrove, J. Reader, W.L. Wiese, and K. Olsen. *NIST Atomic Spectra Database (version 3.1.2)*. National Institute of Standards and Technology, Gaithersburg, MD, 2007.

[22] F. Seitz and D. Turnbull. *Solid State Physics: Advances in research and applications*. Academic Press, 1997.

[23] S. Seung and E. B. Wilson. Ground state energy of lithium and three-electron ions by perturbation theory. *J. Chem. Phys.*, 47:5343–5352, 1967.

[24] C. S. Sharma and C. A. Coulson. Hartree-Fock and correlation energies for 1s2s ^{3}S and ^{1}S states of helium-like ions. *Proceedings of the Physical Society*, 80:81–96, 1962.

[25] J.C. Slater. *Quantum Theory of Atomic Structure*. McGraw-Hill, 1960.

[26] N. Tragin, J.-P. Geindre, C. Chenais-Popovics, J.-C. Gauthier, J.-F. Wyart, and E. Luc-Koenig. Ionization limits in cu-like and ni-like high-z ions from ab initio calculations and wavelength measurements in rydberg series. *Phys. Rev. A*, 39(4):2085–2089, Feb 1989.

[27] K.D. Watson and S.V. ONeil. 1/Z-expansion study of the $1s^22s^2$ ^{1}S, $1s^22s2p$ ^{1}P, and $1s^22p^2$ ^{1}S states of the beryllium isoelectronic sequence. *Phys. Rev. A*, 12(3):729–735, 1975.

[28] S. Wilson. Many-body perturbation theory using a bare-nucleus reference function: a model study. *J. Phys. B: At. Mol. Phys.*, 17:505–518, 1984.

[29] In fact, in Bohr's and Hund's original works [4, 15] the electrons were supposed to occupy hydrogenic Bohr orbits.